Ind. J. Pharm. Edu. Res., 2024; 58(4):1356-1372.
https://www.ijper.org

Original Article

Strategic Targeting of Plasmodium Dihydroorotate Dehydrogenase through Antimicrobial Artemisinin Chiral Centers and their Derivatives: An Integrative Study Using Network Pharmacology and Isothermal Titration Calorimetry

Zia ur Rehman[1,2,*]

[1]Health Research Centre, Jazan University, Jazan, SAUDI ARABIA.
[2]Department of Pharmaceutical Chemistry, College of Pharmacy, Jazan University, Jazan, SAUDI ARABIA.

ABSTRACT

Background: Developing effective antimalarial medications requires understanding the interactions between Plasmodium Dihydroorotate dehydrogenase (DHOdehase) and Artemisinin, including its fourteen stereoisomers (R/S) which have distinct pharmacological effects due to seven chiral centres. **Materials and Methods:** Computational techniques, including molecular docking and network pharmacology, were used to generate and analyse Artemisinin's stereoisomers. The binding strength and durability of the interactions between the stereoisomers and DHOdehase were examined. STRING DB network analysis and pathway enrichment analysis were conducted to identify functional partners and biological pathways associated with DHOdehase. **Results:** The study identified C6 and C8 positions of Artemisinin's stereoisomers as potential binding sites with DHOdehase, showing negative binding energies of -8.7 and -8.2 kcal/mol, respectively. The ligand-protein interactions included hydrogen bonds, Van der Waals forces, Pi-Sigma, alkyl/Pi-alkyl and carbon-hydrogen bonds. STRING DB network analysis revealed DHOdehase interactions with 10 functional partner proteins with confidence scores between 0.889 and 0.999. Pathway enrichment analysis linked DHOdehase to pyrimidine metabolism (KEGG term map00240). Additionally, Isothermal Titration Calorimetry (ITC) demonstrated higher affinity parameters for Artemisinin and its stereoisomer Artesunate. **Conclusion:** The molecular docking, ITC results and network analysis provide insights into the interaction and pharmacological profiles of Artemisinin stereoisomers, laying the groundwork for experimental validation and the development of more effective antimalarial treatments.

Keywords: Malarial Parasite, Plasmodium species, *Artemisia annua*, Artemisinin, Dihydroorotate dehydrogenase, Molecular docking, Network Biology.

Correspondence:
Dr. Zia ur Rehman
[1]Health Research Centre, Jazan University, P.O. Box 114, Jazan-45142, SAUDI ARABIA.
[2]Department of Pharmaceutical Chemistry, College of Pharmacy, Jazan University, P.O. Box 114, Jazan-45142, SAUDI ARABIA.
Email: zrehman@jazanu.edu.sa

Received: 07-09-2024;
Revised: 13-09-2024;
Accepted: 26-09-2024.

INTRODUCTION

Malaria is a mosquito-borne disease infected by distinct Plasmodium parasite species- *P. falciparum*, *P. malariae*, *P. vivax*, *P. knowlesi* and *P. ovale*. Humans contract the parasite when bitten by a carrier Anopheles mosquito.[1] *P. falciparum* accounts for more than 90% of the world's malaria mortality and therefore is a primary parasitic disease and an important global health challenge, particularly in tropical and subtropical countries.[2,3] The World Malaria Report 2023 of the WHO indicated an approx. 300 million cases of malaria, with a considerable number occurring in children (<5 years) worldwide.[4] Malaria remains endemic in over 90 countries, affecting around 40% of the global population.[5] The African states accounted for approximately 94% of all cases of malaria and deaths globally. Additionally, there is a notable incident of malaria imported and instances of local transmission after immigration in North America and Europe, from other non-malarial nations.[6] While malaria is a significant concern, other parasitic diseases also present substantial public health challenges, emphasizing the importance of concerted efforts to manage and get rid of these illnesses for the enhancement of public life and well-being.

Artemisia annua, often known as sweet wormwood, is the plant from which artemisinin is mostly extracted. This compound, classified as a sesquiterpene lactone, features a distinctive

DOI: 10.5530/ijper.58.4.146

endoperoxide bridge (-O-O-), specifically a 1,2,4-trioxane ring, which underlies its antimalarial properties.[7] Apart from malaria, artemisinin and its derivatives have found applications in treating parasitic worm (helminth) infections worldwide.[8] Recent evidence unveils that additionally, powerful immunoregulatory and anti-inflammatory effects are possessed by artemisinin and its derivatives. The notable advantage of artemisinin and its derivatives lies in their established low toxicity, rendering these compounds valuable for chemotherapeutic interventions in human diseases, including Chronic Myeloid Leukemia (CML).[9] Artemisinin has been investigated in clinical trials exploring its efficacy in treating conditions such as schizophrenia, malaria and specifically falciparum malaria. Furthermore, artemisinin and Artesunate exhibits antiviral properties and has been effectively evaluated as a treatment for Hepatitis B Virus (HBV).[10] Recent findings indicate that dihydroartemisinin possesses angiogenic activity.

Artemisinin, along with its semi-synthetic derivatives, constitutes a class of antimalarial drugs utilized in treating malaria. These drugs exert their effects against Plasmodia at various stages in their life cycle within humans. Globally recognized as the standard treatment for *P. falciparum* malaria and other Plasmodium species, Artemisinin-based Combination Therapies (ACTs) are preferred. The WHO explicitly discourages the use of artemisinin as monotherapy due to concerns about emerging drug resistance in malarial parasites. Contemporary treatment regimens involve blending artemisinin or its chemical derivatives with prescription drugs that treat malaria. The advantages of ACTs include rapid parasite elimination and efficacy across various stages of the parasite life cycle. However, challenges such as low bioavailability, suboptimal pharmacokinetic properties and elevated costs are associated with these treatments.

After extensive survey of Drug Bank (https://go.drugbank.com/) we have selected five Artemisinin derivatives, that constitutes a class of antimalarial drugs are Artesunate (DB09274), Artemether (DB06697), Artemotil or Beta arteether or Artecef (DB13851), Dihydroartemisinin or Artenimol (DB11638) and Artemisitene (D0C1PB). Artesunate, a derivative of artemisinin, is recommended as the favourite drug for treatment for severe malaria. It has gained endorsement from the WHO as the first line of treatment for severe malaria, addressing the need for a more hydrophilic artemisinin derivative.[8,11] For treating uncomplicated acute, malaria by infected *P. falciparum*, artemether, typically utilized in combination of lumefantrine is first choice. Administered in combination with lumefantrine, this therapy enhances efficacy against the erythrocytic stages of various Plasmodium species. It is equally effective against parasites acquired in chloroquine-resistant infection zones. Artemotil (a semi-synthetic) derivative of artemisinin, specifically designed as a fast-acting killer of the parasites in schizont stage in RBC (blood schizonticide). It is recommended for the treatment of cerebral malaria cases and *P. falciparum* malaria that is resistant to chloroquine. Artenimol, another artemisinin derivative, functions as an antimalarial agent for treating uncomplicated *P. falciparum* infections. Approved by the European Medicines Agency (EMA), it is available combined with piperaquine with a brand name Eurartesim. The WHO advises artenimol as part of an ACT (Artemisinin Combination Therapy) since it is a very effective treatment for malaria.

Similarly, an extensive survey of the Therapeutic Target Database (TTD) available at https://db.idrblab.net/ttd/ unveils that there are several well-known antimalarial drug target proteins of *Plasmodium falciparum* parasite. TTD is a database that offers insights on the intended disease, known and described therapeutic protein and nucleic acid targets, information regarding pathways and medications that are specifically focused on each of these targets. The first one is Plasmodium DHOdehase, which is critical for the conversion of (S)-dihydroorotate to orotate during UMP biosynthesis via de novo pathway of pyrimidine metabolism of the parasite (Figure 1).[12-15]

Plasmodium DHOdehase is a Class 2 enzyme (Enzyme Commission No. 1.3.5.2) present in eukaryotes within the mitochondrial membrane and contains FMN.[16,17] DHOdehase performs Oxidoreductase reactions (1.), operating on the CH-CH group (1.3) of donors, with a quinone or similar molecule (1.3.5) as an acceptor. Therefore, it falls under the classification of the Class two dihydroorotate dehydrogenase (DHOdehase) enzyme. The only redox process involved in the de novo production of pyrimidine nucleotides is this enzymatic reaction. [16,18] Ubiquinone-6 and -7 are the enzyme's most efficient quinone electron (e-) acceptors. However, simpler quinones (e.g. Benzoquinone), can also behave as electron (e-) acceptors, albeit with reduced pace. Substrates for the enzyme include benzyl (S)-dihydroorotates, ethyl-, methyl- and tert-butyl.[16,18] It's important to mention that Class 1 DHOdehase enzyme utilize NAD+ (EC 1.3.1.14), or NADP+ (EC 1.3.1.15) and fumarate (EC 1.3.98.1), as electron acceptors (Figure 1). Hence, there is a compelling need to explore the binding capabilities of the stereoisomers of Artemisinin along with its five derivatives against the Dihydroorotate dehydrogenase of the Plasmodium parasite. This investigation aims to conduct a comprehensive assessment of the molecular and atomic-level interactions between the ligands and the protein of interest.

MATERIALS AND METHODS

Ligand Preparation

The structures of artemisinin (CID:68827) and its five derivatives-Artemisitene (CID:11000442), Artemether (CID: 68911), Artemotil or Beta arteether or Artecef (CID: 3000469), Dihydroartemisinin or Artenimol (CID: 3000518), Artesunate (CID: 6917864) were retrieved from PubChem (https://pubchem.ncbi.nlm.nih.gov/) and manually drawn in ChemDraw

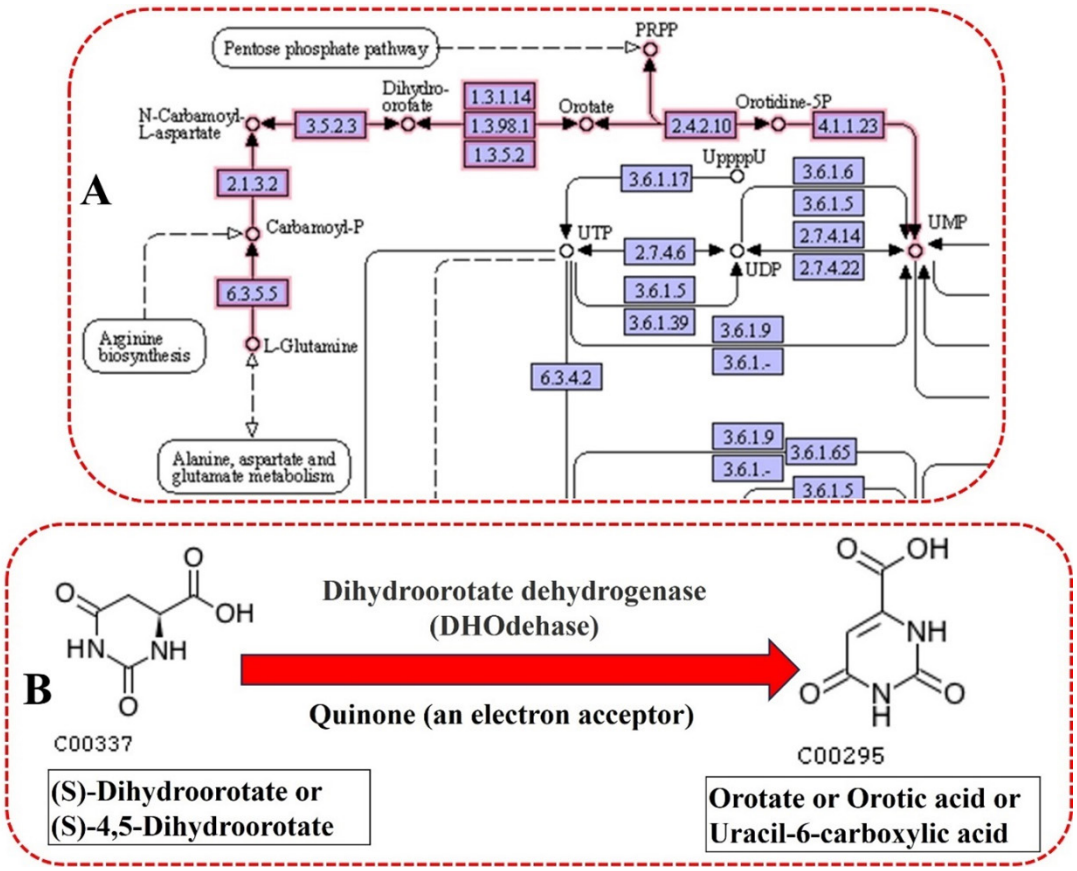

Figure 1: (A) The De novo UMP biosynthesis from L-Glutamine to Uridine 5′-Monophosphate (UMP) during the pyrimidine biosynthesis pathway (the route is highlighted in red). The sole redox process involved in the de novo synthesis of pyrimidine nucleotides, specifically Uridine 5'-Monophosphate (UMP), is enzymatic. This Class two DHOdehase enzyme [EC:1.3.5.2] uses quinone (ubiquinone-6 and ubiquinone-7) as best electron acceptors for the enzyme, simpler quinones (eg. Benzoquinone), can also behave as electron (e-) acceptors, albeit with reduced pace. The Class one DHOdehase use NADP+ (EC1.3.1.15) fumarate (EC1.3.98.1), or NAD+ (EC1.3.1.14), as an electron acceptor. (B) During UMP biosynthesis via the de novo pathway DHOdehase catalyzes the conversion of (S)-dihydroorotate (C00337) to orotate or Orotic acid (C00295) with quinone as an electron acceptor.

Professional version 16.0.1.4 (Figure 2). The fourteen stereoisomers (R/S) of Artemisinin as ligands were also manually drawn in ChemDraw Professional version 16.0.1.4 (77) for molecular docking studies (Figure 3). Furthermore, advanced computational tools were used to verify the different stereoisomers and ensure accurate representation in PyMol and PMV.

Drug Structure Similarity Search for Artemisinin in TTD and DB

Drug structure similarity searching relies on the Tanimoto similarity searching method. The process begins with an input compound structure provided in MOL, SDF, or SMILES format, which is then transformed into a vector comprising molecular descriptors utilizing cheminformatics tools ChemAxon software. Molecular descriptors serve as quantitative representations of the structural and physicochemical features of molecules. These descriptors have been widely employed in the development of Structure-Activity Relationships (SAR), virtual screening and Quantitative Structure-Activity Relationships (QSAR) tools for drug discovery.

Human Proteins Similarity searching

The selection of *P. falciparum* Dihydroorotate dehydrogenase (amino acid 158-569) as an ideal target is based on a BLASTp similarity search comparing its sequence with all proteins of Homo sapiens (taxid:9606). In this analysis, similarity proteins for the target are defined by having an E-value less than 0.005 and employing the BLOSUM62 matrix outside the protein families of the target. The absence of similarity proteins with human sequences (E-value < 0.005) for this target indicates a lack of significant sequence similarity with human proteins. This trait is advantageous in drug development, as it indicates a decreased probability of unwanted interactions, hence improving the potential for developing effective drugs.[19]

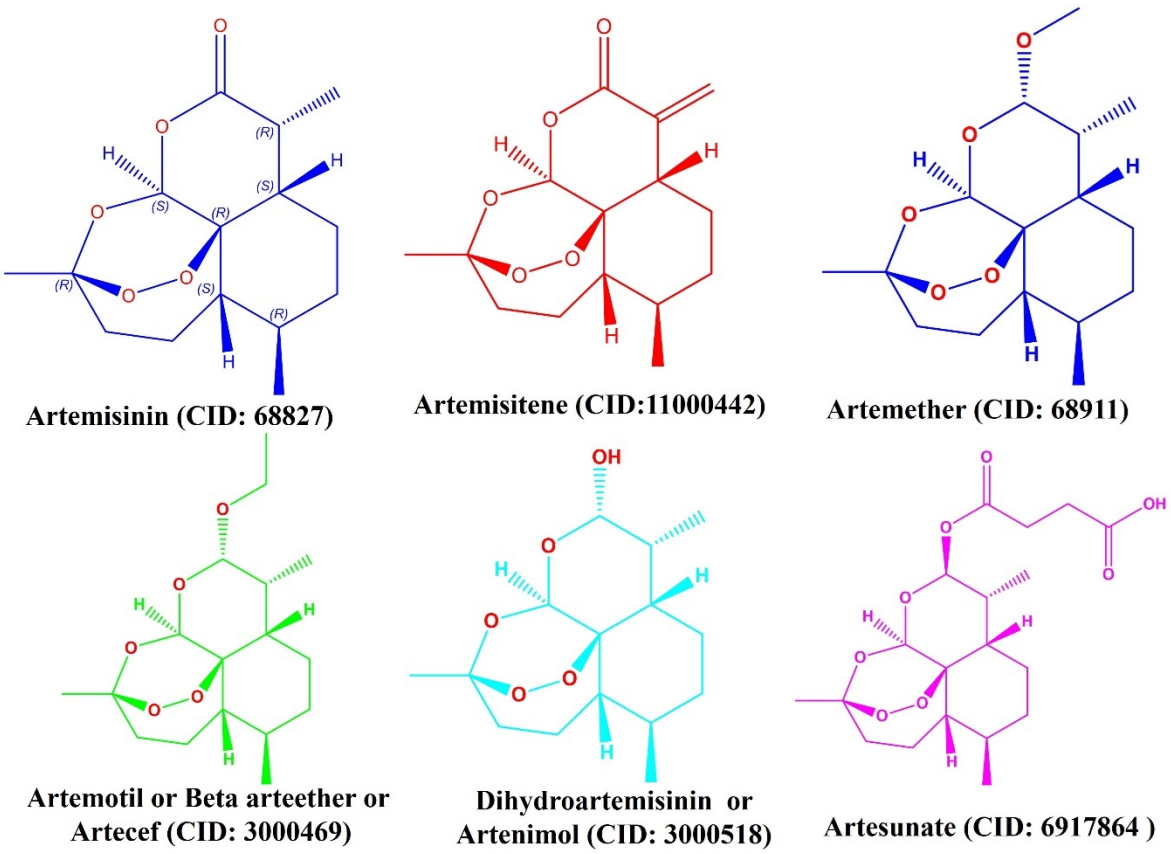

Figure 2: Molecular structures of artemisinin (CID: 68827) and its five derivatives are depicted, illustrating their respective features. Artemisitene (CID: 11000442) is characterized by the absence of active torsion. Artemether (CID: 68911) exhibits a single active torsion in its structure. Artemotil, also known as Beta-arteether or Artecef (CID: 3000469), displays two active torsions. Dihydroartemisinin or Artenimol (CID: 3000518) possesses two active torsions as well. In contrast, Artesunate (CID: 6917864) structure exhibits a maximum of six active torsions, as identified by AutoDock Ligand analysis.

Protein Structure Retrieval

The therapeutic target protein Plasmodium DHOdehase (PDB ID: 1TV5, Target ID: T01318), 3D structure was obtained from the most dependable the Protein Data Bank (PDB).

Binding pocket prediction

The active site of Plasmodium DHOdehase (PDB ID: 1TV5) was identified using the CASTp (http://sts.bioe.uic.edu/castp/index.html?201l) version 3.0 web server.[20] The CASTp server used the default probe radius of 1.4 Angstroms.

Molecular docking and Binding Energy Calculation

Virtual screening through molecular docking was executed with the help of AutoDock-Vina version 4.2.[21-23] Gasteiger-Marsili partial charges were provided to the ligand molecules (.PDB format) and converted them to PDBQT format. The polar hydrogen atoms were added to target Plasmodium Dihydroorotate dehydrogenase (PDB IDP: 1TV5) protein with subsequently energy minimized by removing water molecules, heteroatoms, form crystal structure. The charge deficiency on target protein was then dispersed using partial atomic Kollman charges. Finally, the PDB files of ligands and protein was transformed to dot PDBQT format.[24,25] Employing AutoDock Tools (version-1.5.7), grid box with X-, Y- and Z-dimensions was constructed.

LigPlot Plus version-1.4.5,[26] was employed to identify the amino acid residues of target protein directly involved in the atomic level interactions with ligands. Based on contributions from Hydrogen (H-) bonds, ionic bonds, hydrophobic contacts and Van Der Waals (VDW) interactions between the ligand (inhibitor) and target (protein), we calculated the mean free energy (ΔG), which represents the docking affinity scoring. The protein-ligand complexes were then displayed using the PyMOL Molecular Graphics System, Version 2.0[22] and Discovery Studio visualizer.[27]

Network biology for Prediction of Functional Partners

To achieve the intended objective, the UniProt Accession No. Q08210 corresponding to Dihydroorotate Dehydrogenase of *P. falciparum* was employed as a query in the STRING DB, a comprehensive biological database and online resource for intraprotein interactions.[28] This resource integrates diverse data sources, including computational predictions, experimental

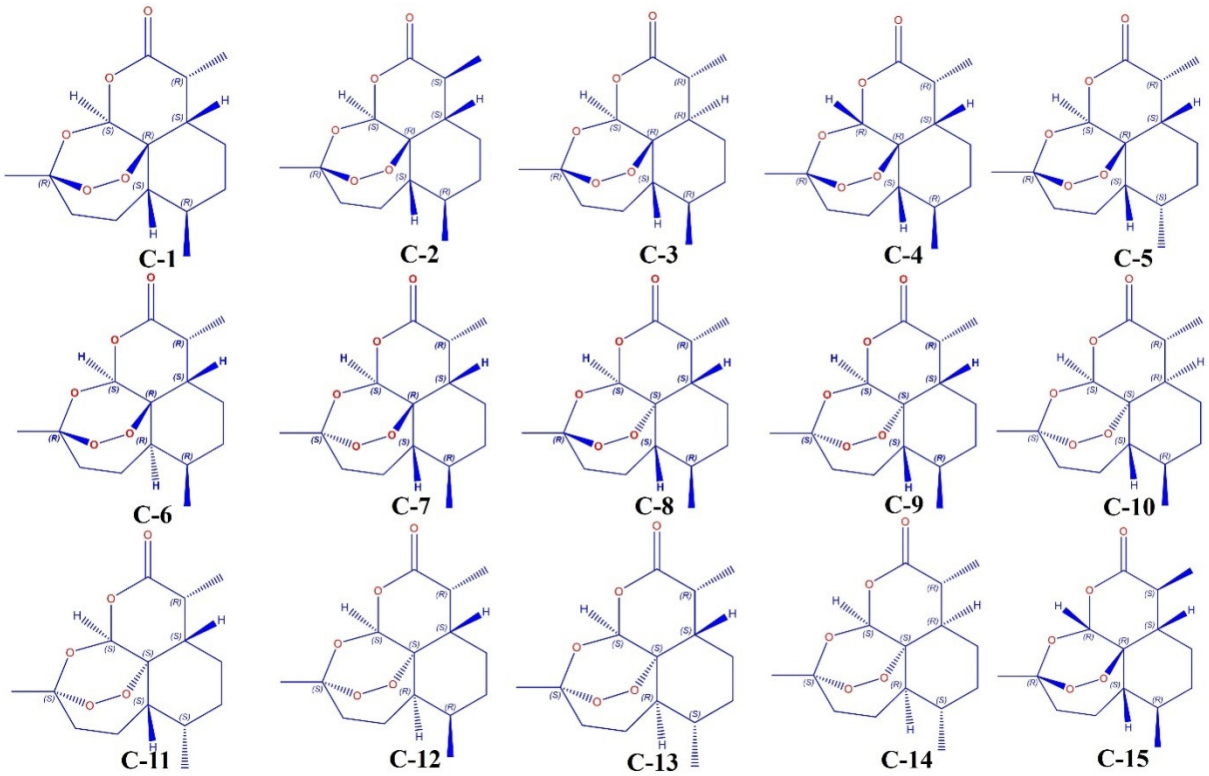

Figure 3: Artemisinin features seven specified stereocenters (R/S), giving rise to fourteen stereoisomers. These stereogenic centers, denoted as C1-C15, involve carbon atoms bonded to four distinct substituents. The terms "R" and "S" correspond to the "rectus" (right) and "sinister" (left) configurations of chiral centers, respectively. Notably, all stereoisomers of Artemisinin, lack active torsions as identified by AutoDock analysis.

findings and publicly available text collections, ensuring regular updates. Utilizing STRING database (https://version-11-5.string-db.org/), a K-means clustering approach was implemented to categorize the Protein-Protein Interaction (PPI) network into three distinct groups. The medium confidence score of 0.400 was configured to visualize the complete STRING network, illustrating functional and physical associations among target and database proteins. Interaction evidence types were indicated by line color, data support level by line thickness and cluster borders by dotted lines. The line colors denoted interaction evidence types such as databases, text mining, neighborhood, experiments, coexpression, gene fusion and cooccurrence, while magenta and purple edges represented experimentally discovered and curated database-derived Gene-Gene Interactions (GGI), respectively. Red, green and blue edges signified predicted gene-gene interactions through gene fusions, neighborhood and cooccurrence, respectively. The PPI network, delineated by nodes and edges, was further analyzed for functional enrichments using classification systems like GO, Pfam and KEGG.[29,30] Bar graphs were constructed using Microsoft Office Excel 2010.[31]

Enrichment of GO annotation and KEGG pathways

STRING DB version 11.5 was employed for GO annotation (Cellular Component-CC, Biological Process-BP and Molecular Function-MF) and KEGG pathway enrichment analyses to unravel the functional insights and metabolic pathways associated with *P. falciparum* Dihydroorotate Dehydrogenase in the context of controlling other pathogenic proteins. Meanwhile, KEGG and Reactome pathway analysis aimed to identify critical metabolic pathways crucial for the survival and pathogenicity of *P. falciparum*. To ensure robust results, GO terms and KEGG pathways with a Log10 *p*-value less than 0.001, a low False Discovery Rate (FDR) and a high prediction strength (>0.5) were meticulously shortlisted, highlighting statistically significant and biologically relevant annotations and pathways.

Isothermal Calorimetry (ITC)

Dihydroorotate Dehydrogenase's affinity for ligands (Artemisinin and its derivatives Artemisitene, Artemether, Artemotil, Dihydroartemisinin or Artenimol and Artesunate) was investigated using Isothermal Titration Calorimetry (ITC). The highest grade of Dihydroorotate Dehydrogenase's and inhibitors, which include artemisinin and its derivatives, artemisitene, artemotil, dihydroartemisinin, or artenimol and artesunate, were obtained from Sigma Aldrich for the ITC measurement. As previously mentioned, isothermal titration calorimetric measurements were made using a Malvern Instruments (Malvern, UK) device at 25°C and pH 7.5 (ITC buffer) (Damian 2013). Here, the concentration of protein and ligands was measured spectrophotometrically using standard

Table 1: Drug structure similarity result for input Artemisinin in Therapeutic Target Database (TTD) and Drug Bank (DB) with Tanimoto Similarity (>0.7).

Drug ID	PubChem Chemical ID	Drug Name	Drug type categories or Status	Tanimoto Similarity	Type of Similarity
D0S3WH	68827	Artemisinin	Investigational	1.0	High-similarity
D0D4JO	6917864	Artesunate	Approved, Investigational	0.876	High-similarity
D0C1PB	11000442	Artemisitene	Nutraceutical	0.843	Intermediate-similarity
D0M9BW	68911	Artemether	Approved	0.842	Intermediate-similarity
D0Y5ZA	3000469	Artemotil	Approved	0.842	Intermediate-similarity
D0N6FH	3000518	Artenimol or Dihydroartemisinin	Approved, Investigational, Experimental	0.810	Intermediate-similarity

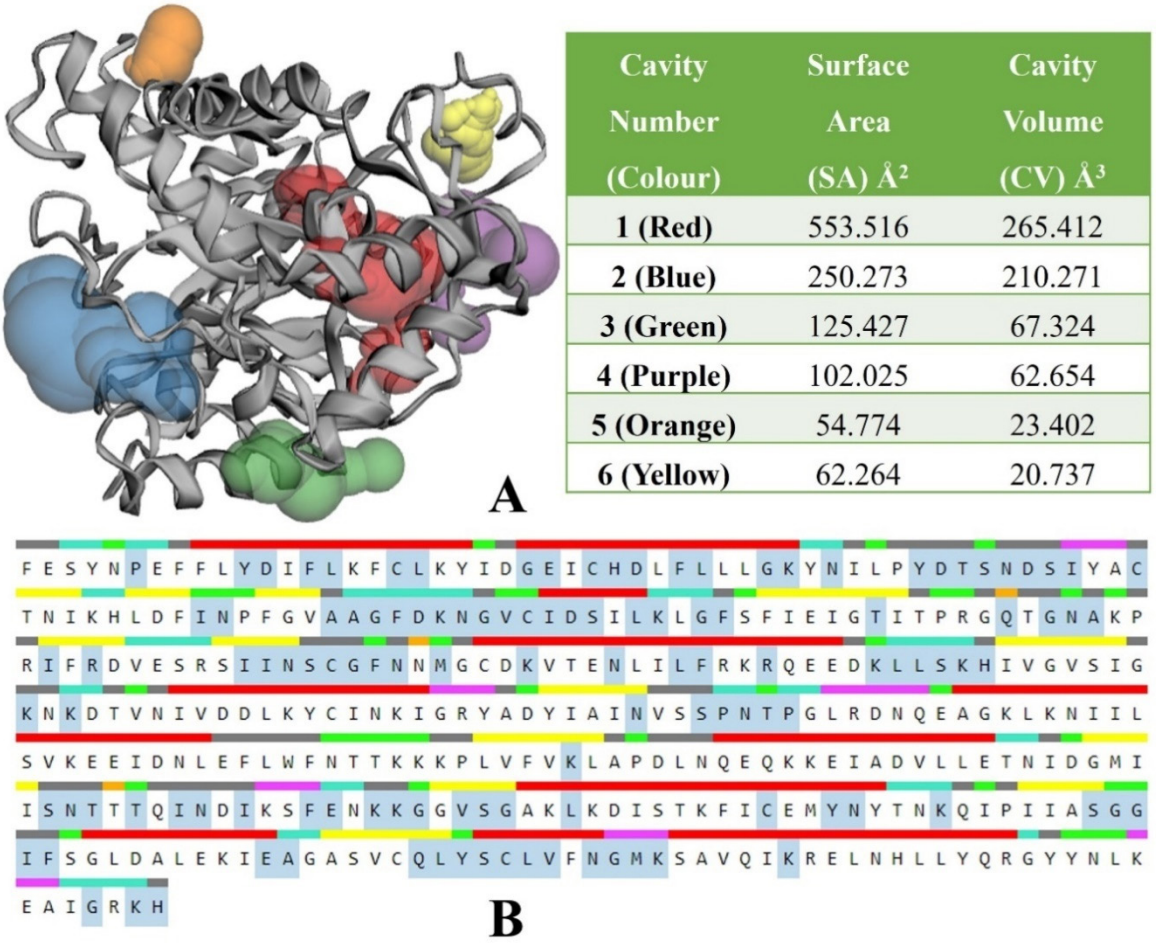

Figure 4: (A) Prediction of binding pockets in Plasmodium Dihydroorotate Dehydrogenase (PDB ID: 1TV5) was conducted using the CASTp server, revealing six distinctive cavities designated by color-coding: red (Cavity 1), blue (Cavity 2), green (Cavity 3), purple (Cavity 4), orange (Cavity 5) and yellow (Cavity 6). Each cavity is characterized by specific surface areas and volumes, with Cavity 1, highlighted in red, exhibiting the largest SA of 553.516 Å^2 and a substantial V of 265.412 Å^3. (B) The amino acid residues constituting Cavity 1 (red), Cavity 2 (blue), Cavity 3 (green), Cavity 4 (purple), Cavity 5 (orange) and Cavity 6 (yellow) are distinctly highlighted with different colors, providing insights into the structural features of each cavity.

reference extinction coefficients. Dihydroorotate Dehydrogenase and inhibitors (Artemisinin and derivatives Artemisitene, Artemether, Artemotil, Dihydroartemisinin or Artenimol and Artesunate) were dissolved in the ITC buffer 5 mM HEPES-KOH, pH 7.5. The putative ligands (Artemisinin and its derivatives, Artemisitene, Artemether, Artemotil, Dihydroartemisinin or Artenimol and Artesunate) were used in different ITC studies and measurements for Dihydroorotate Dehydrogenase, where

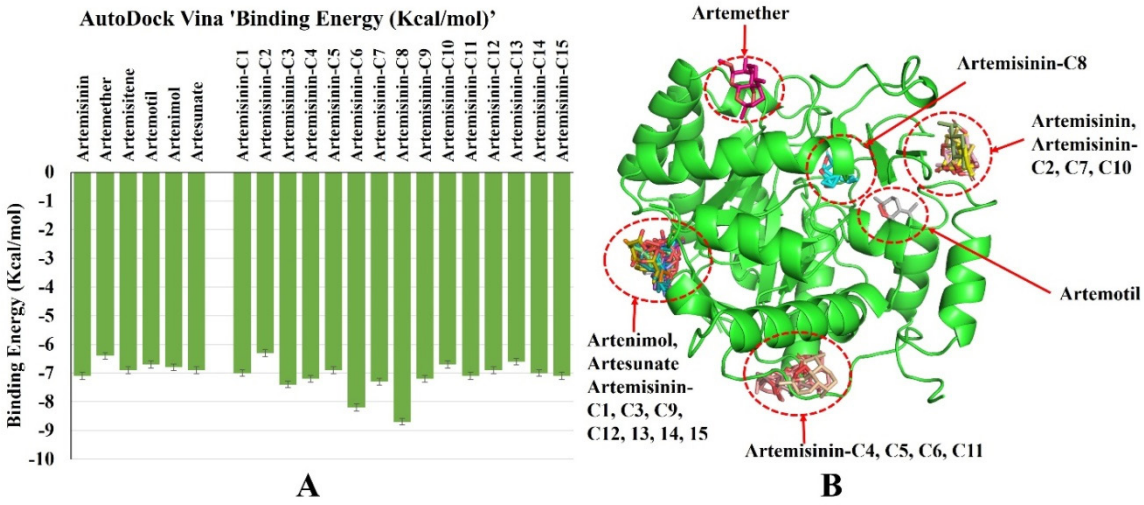

Figure 5: (A) The binding energies (Kcal/mol) of Artemisinin, Artemether, Artemisitene, Artemotil, Artenimol, Artesunate and the fourteen stereoisomers of Artemisinin C1-C15 complexed with Plasmodium Dihydroorotate dehydrogenase (PDB ID: 1TV5) were assessed using AutoDock Vina. (B) The illustration of Plasmodium DHOdehase (PDB ID: 1TV5) shows the six binding cavities that are accessible to the stereoisomers of artemisinin (C1-C15) and their derivatives.

ligands were permitted to bind with numerous binding sites. In this case, ITC measurements were limited to ligands that were screened and virtually evaluated, specifically artemisinin and its derivatives, artemisitene, artemotil, dihydroartemisinin, or artenimol and artesunate.

RESULTS

Drug Structure Similarity Search

In the Therapeutic Target Database (TTD) and Drug Bank (DB) search, Artemisinin (CID: 68827) is classified as Investigational and exhibits a Tanimoto Similarity of 1.0, indicating high similarity. The cheminformatics tools ChemAxon was employed to calculate Tanimoto similarity scores (Table 1). Artesunate (CID: 6917864), categorized as Approved and Investigational, shows a Tanimoto Similarity of 0.876, reflecting high similarity. Artemisitene (CID: 11000442), classified as Nutraceutical, demonstrates an intermediate similarity with a Tanimoto Similarity of 0.843. Artemether (CID: 68911) and Artemotil (CID: 3000469), both approved drugs, share an intermediate similarity with Tanimoto Similarities of 0.842. Artenimol or Dihydroartemisinin (CID: 3000518), designated as Approved, Investigational and Experimental, exhibits an intermediate similarity with a Tanimoto Similarity of 0.810 (Table 1). These results highlight the structural relationships between Artemisinin and related compounds, providing insights into their chemical similarities and diverse drug statuses.

Analysis of Binding pocket

The results reveal the characteristics of six distinct cavities identified by color-coding: red (Cavity 1), blue (Cavity 2), green (Cavity 3), purple (Cavity 4), orange (Cavity 5) and yellow (Cavity 6) (Figure 4 A and B). Each cavity is characterized by specific surface areas and volumes. Cavity 1, marked in red, exhibits the largest surface area (SA) of 553.516 Å^2 and a substantial volume (V) of 265.412 Å^3. Cavity 2, designated in blue, features a surface area of 250.273 Å^2 and a voluminous 210.271 Å^3. Green Cavity 3 encompasses a SA of 125.427 Å^2 and a V of 67.324 Å^3. Purple Cavity 4 is defined by a SA of 102.025 Å^2 and a V of 62.654 Å^3. Orange Cavity 5 displays a SA of 54.774 Å^2 and a V of 23.402 Å^3. Lastly, yellow Cavity 6 presents a SA of 62.264 Å^2 and a V of 20.737 Å^3. These quantitative measurements provide a comprehensive understanding of the structural attributes of each cavity.

Computational Molecular Docking Analysis

Docking is a computer method used to forecast the most favourable arrangement of two molecules when they bind together to create a stable complex. The preferred orientation of one molecule to another is predicted via molecular docking when bonded to create a stable complex. The AutoDock binding energies (Kcal/mol) were determined for Artemisinin and its stereoisomers and derivatives in complex with Plasmodium Dihydroorotate dehydrogenase. Artemisinin exhibited a binding energy (delta G) of -7.1 Kcal/mol, while Artemether, Artemisitene, Artemotil, Artenimol and Artesunate displayed very slight change in binding energies of -6.4, -6.9, -6.7, -6.8 and -6.9 Kcal/mol, respectively (Figure 5 A).

The AutoDock binding energies (Kcal/mol) for various stereoisomers of Artemisinin in complex with Plasmodium Dihydroorotate dehydrogenase were determined quantitatively. Artemisinin stereoisomers displayed diverse binding energies, ranging from -6.3 to -8.7 Kcal/mol. Notably, Artemisinin C6 and C8 exhibited exceptionally high binding affinities of -8.2 and -8.7

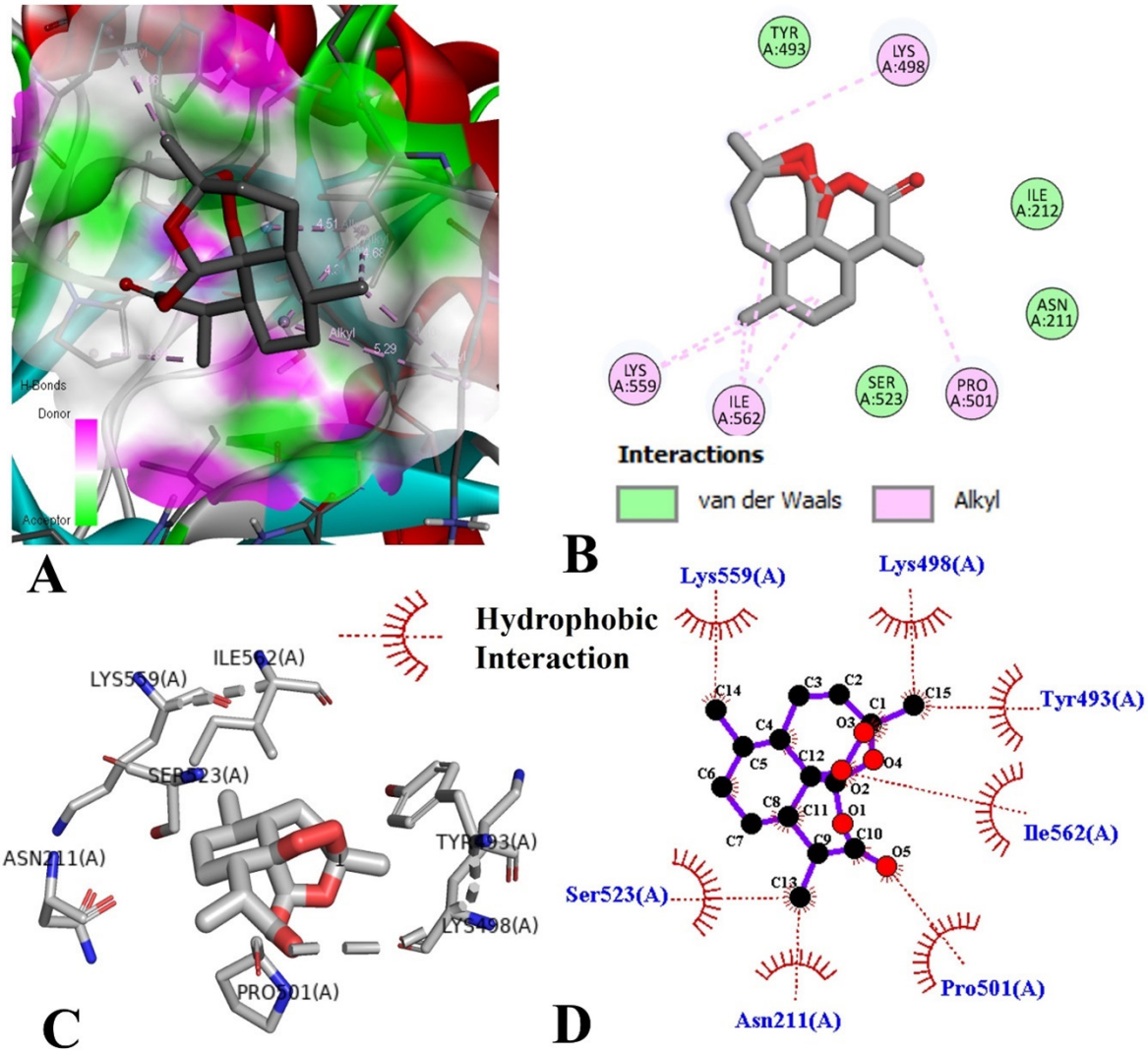

Figure 6: Docked complexes involving the Plasmodium Dihydroorotate dehydrogenase (PDB ID: 1TV5) protein and native form artemisinin. (A) Hydrogen-bond donor and acceptor interacting residue between the DHOdehase and the ligand Artemisinin (gray) are shown. The expanded image displays the bond length as well as the residues of the donor and acceptor hydrogen (H-) bond in the binding cavity. (B) Potential active site residues forming separate Van der Waals (ASN211, ILE212, TYR493 and SER523) and alkyl (LYS498, PRO501, LYS559 and ILE562) interactions were also indicated using Discovery Studio 2D diagrams. (C) The PyMol 3D image demonstrates a crucial interaction between functionally relevant residues and artemisinin (gray). (D) The LigPlot+ shows that the 2D Discovery Studio diagram and the hydrophobic interacting amino acid residue of the binding cavity are identical.

Kcal/mol (Figure 5 A), suggesting a robust interaction with the target protein. These quantitative values provide a comprehensive assessment of the binding strengths of different Artemisinin stereoisomers, indicating potential variations in their inhibitory capacities against Plasmodium Dihydroorotate dehydrogenase.

Docking investigation showed Artemisinin-C8 and Artemotil were docked in cavity No. 1, which had the biggest surface area (553.516 Å^2) and volume (265.412 Å^3). It was also found that Artenimol, Artesunate, Artemisinin and seven of its stereoisomers (C1, C3, C9, C12, 13, 14, 15) were docked in the second-largest cavity (Cavity No. 2), which has a SA of 250.273 Å^2 and a V of 210.271 Å^3 (Figure 5B). These results provide information about the drugs' interactions and affinities with the target binding site, implying their efficacy in inhibiting Plasmodium DHOdehase.

Docking Artemisinin with DHOdehase (PDB ID: 1TV5) yielded important insights into molecular level interactions. The docking simulations uncover specific amino acid residues involved in hydrogen bonding, emphasizing the critical role of residues within the binding cavity. Discovery Studio 2D diagrams highlight the presence of active site residues, showcasing Van der Waals (ASN211, ILE212, TYR493 and SER523) and alkyl (LYS498, PRO501, LYS559 and ILE562) interactions that contribute to the stability of the Artemisinin-DHOdehase complex. This molecular insight is further substantiated by PyMol 3D images, providing a visual representation of the significant interactions between

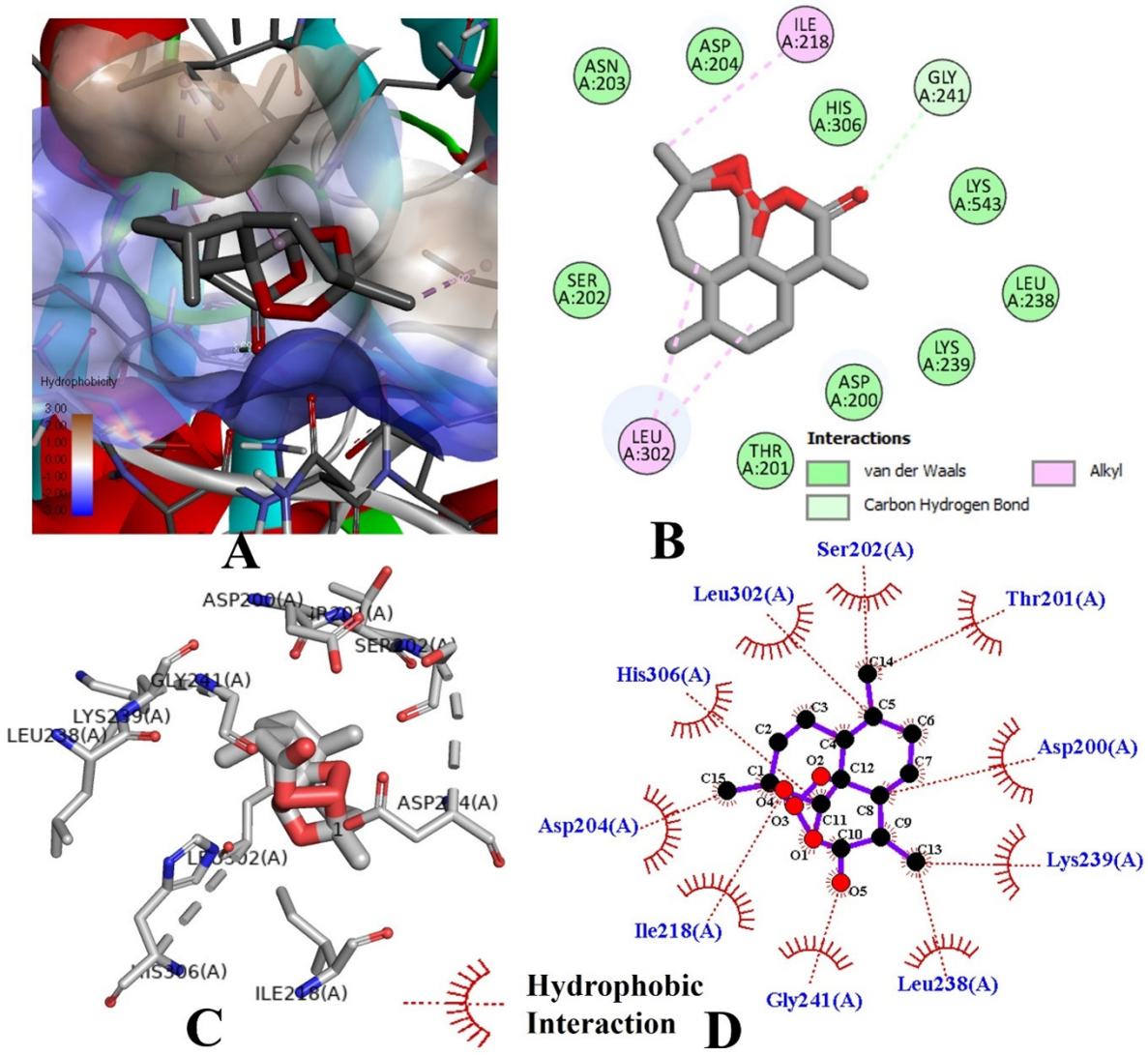

Figure 7: Docked complexes of Plasmodium Dihydroorotate dehydrogenase (PDB ID: 1TV5) with Artemisinin-stereoisomer C6. (A) The hydrophobicity of cavity residues is used to illustrate the interactions between DHOdehase and the ligand Artemisinin-stereoisomer C6 (gray). (B) Potential active site residues were identified by Discovery Studio 2D diagrams as separate Van der Waals (ASP200, THR201, SER202, ASN203, ASP204, HIS306, LEU238, LYS239 and LYS543), alkyl (ILE218 and LEU302) and carbon-hydrogen bond interactions (GLY241). (C) The PyMol 3D picture demonstrates how essential residues and artemisinin C6 (gray) interact significantly. (D) The LigPlot+ and 2D Discovery Studio diagram both display the same binding cavity's hydrophobic interacting amino acid residue.

Artemisinin and functionally important residues in the protein. LigPlot+ analysis aligns with the 2D diagrams, emphasizing the hydrophobic interacting amino acid residues within the binding cavity (Figure 6 A-D).

The docking analysis of Artemisinin-stereoisomer C6 with Plasmodium Dihydroorotate Dehydrogenase (PDB ID: 1TV5) provides a detailed insight into the molecular interactions at the binding site. The interaction profiles are illustrated in Figure 7. The enlarged image emphasizes the hydrophobic nature of amino acid residues within the binding cavity, showcasing bond lengths. Discovery Studio 2D diagrams further elucidate the active site residues, emphasizing Van der Waals interactions with specific amino acids such as ASP200, THR201, SER202, ASN203, ASP204, HIS306, LEU238, LYS239 and LYS543. Additionally, alkyl interactions involving ILE218 and LEU302 are highlighted, while GLY241 exhibits carbon-hydrogen bond interactions. The PyMol 3D image visually represents the significant interactions between Artemisinin-stereoisomer C6 and functionally important residues in the protein. LigPlot+ analysis complements the 2D Discovery Studio diagram by emphasizing the hydrophobic interacting amino acid residues within the binding cavity. This detailed molecular understanding sheds light on the specific binding mode of Artemisinin-stereoisomer C6 with Plasmodium Dihydroorotate Dehydrogenase, providing essential information for potential drug-target interactions.

Artemisinin-stereoisomer C8, when docked with Plasmodium Dihydroorotate Dehydrogenase (PDB ID: 1TV5), exhibits remarkable interactive and inhibitory potential, as evidenced by

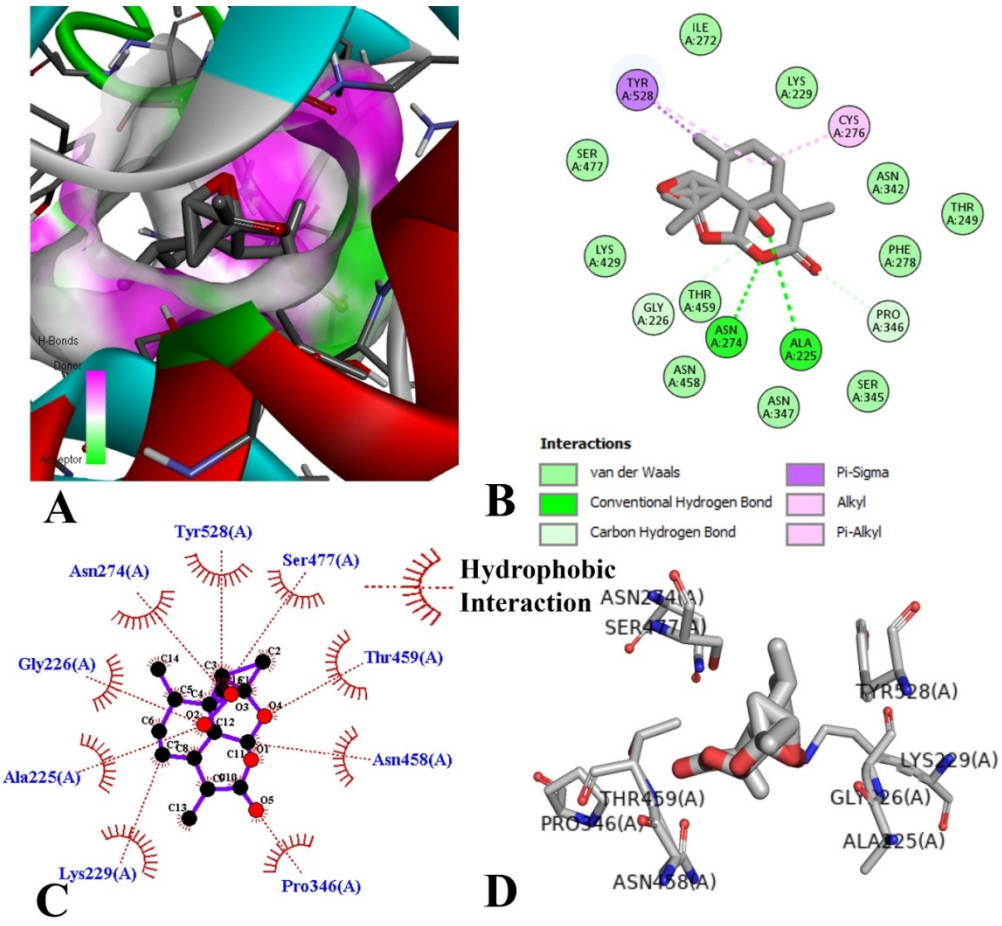

Figure 8: Docked complexes of the Plasmodium dihydroorotate dehydrogenase (PDB ID: 1TV5) protein with Artemisinin-stereoisomer C8. (A) The hydrogen-bond donor and acceptor interacting residue between the DHOdehase and the Artemisinin-stereoisomer C8 (gray) are shown. The expanded image displays the bond length as well as the residues of the donor and acceptor hydrogen bond in the binding cavity. (B) Possible active site residues were also shown by Discovery Studio 2D diagrams, indicating unique Van der Waals (LYS229, THR249, ILE272, PHE278, PHE278, SER345, ASN342, LYS429, ASN347, ASN458, THR459 and SER477), Hydrogen bonds (ALA225, ASN274), alkyl/Pi-alkyl (CYS276), Pi-Sigma (THr528) while PRO346 shows carbon-hydrogen bond interactions. (C) LigPlot+ shows a similar hydrophobic interacting amino acid residue of the binding cavity but shows less no. of amino acid residues as compared to the 2D Discovery Studio diagram. (D) The PyMol 3D image shows a significant interaction of Artemisinin C8 (grey) with functionally important residues.

diverse molecular interactions. The docked complex's detailed analysis is presented in Figure 8, showcasing the interactions between Dihydroorotate Dehydrogenase (DHOdehase) protein and Artemisinin-stereoisomer C8. This interaction is highly interactive and productive in terms of inhibitory potential, as it forms H-bonds, C-H bonds, van der Waals (VDW), Pi-Sigma, Alkyl and Pi-Alkyl interactions.

The interactions include hydrogen-bonding interactions with specific donor and acceptor residues within the binding cavity, as depicted in the enlarged image highlighting bond lengths. Discovery Studio 2D diagrams provide further insights into potential active site residues, emphasizing distinct Van der Waals interactions with amino acids such as LYS229, THR249, ILE272, PHE278, SER345, ASN342, LYS429, ASN347, ASN458, THR459 and SER477. Hydrogen bond interactions involve ALA225 and ASN274, while alkyl/Pi-alkyl interactions with CYS276 and Pi-Sigma interactions with THR528 contribute to the complex network of binding interactions. Additionally, PRO346 shows carbon-hydrogen bond interactions (Figure 8 A-D). LigPlot+ analysis and PyMol 3D images complement the 2D Discovery Studio diagram, providing a comprehensive view of the hydrophobic interacting amino acid residues within the binding cavity. This thorough molecular characterization underscores the potential inhibitory efficacy of Artemisinin-stereoisomer C8 against Plasmodium Dihydroorotate Dehydrogenase, contributing valuable information to the understanding of anti-malarial mechanisms. Understanding these molecular interactions is crucial for deciphering the binding mechanism and potential inhibitory effects of Artemisinin on Plasmodium Dihydroorotate dehydrogenase. The significance lies in unraveling potential drug-target interactions, offering valuable information

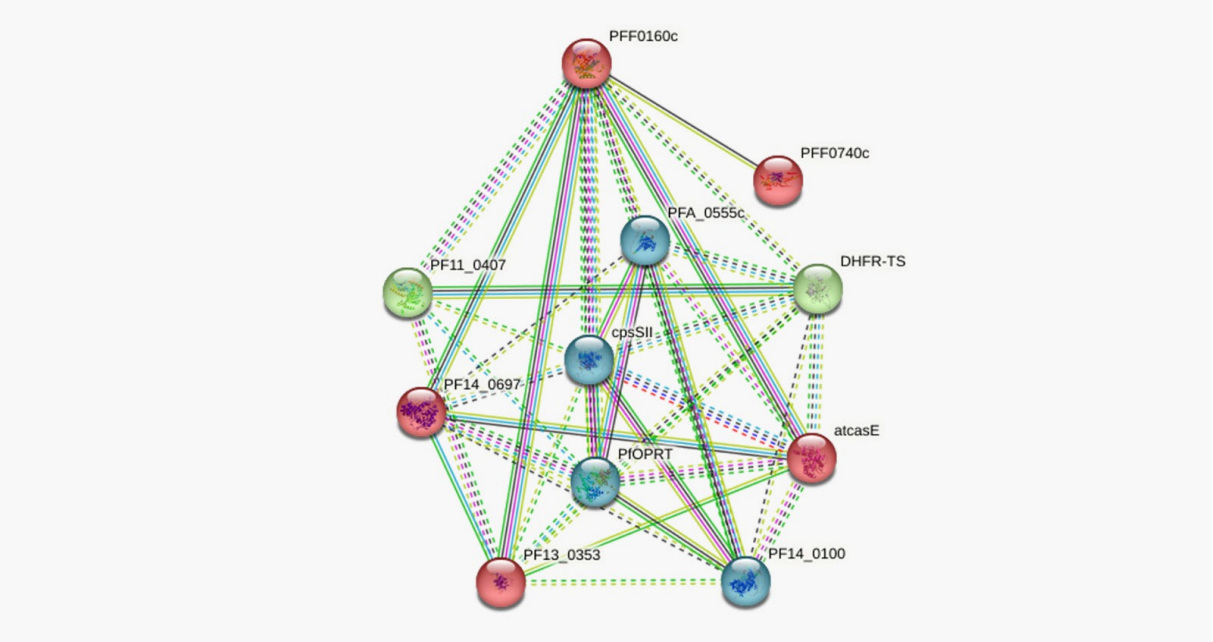

Figure 9: Dihydroorotate dehydrogenase (Protein Symbol: PFF0160c) and ten Predicted Functional Partners in the intrapathogen PPI network. Whereas purple edges show known GGI from carefully curated databases, magenta edges show Gene-Gene Interactions (GGI) that have been found through experimentation. The expected GGI are represented by green edges (neighbourhood), red edges (fusions) and blue edges (cooccurrence), in that order.

for the development of anti-malarial strategies and advancing our understanding of the molecular basis of Artemisinin's anti-malarial activity.

Network biology for Prediction of Functional Partners of Dihydroorotate dehydrogenase Dihydroorotate dehydrogenase (UniProt ID: Q08210 and Protein Symbol: PFF0160c) of *P. falciparum* (NCBI taxonomy ID:5833) interacts with ten functional Partner proteins as revealed by STRING Data base version 11.5 (Figure 10 and Table 4). Here are 40 edges that bind 11 nodes together. The node has a very high average degree of 7.27, a mean local clustering coefficient (LCC) of 0.892 and a PPI-enrichment *p*-value of 6.86e-09, indicating that it is sufficiently connected to control the network. Based on the degree of contacts, the PPI network comprising 11 proteins created its three K-mean clusters. The I level of interactors are represented by the red cluster of five nodes (PF13_0353, PF14_0697, PFF0160c, PFF0740c and atcasE), the II level of interactors are green cluster of two nodes (DHFR-TS and PF11_0407) and the III level of interactors are blue cluster of four nodes (PF14_0100, PFA_0555c, PfOPRT and cpsSII) (Figure 9). Within the larger PPI network, these clusters, which are composed of protein groups with increased connection among themselves, constitute coherent subnetworks. The network displays a densely packed and well-connected interaction network, as evidenced by its high local clustering coefficient and average node degree. The PPI enrichment *p*-value indicates that the observed interactions are much larger than what would be predicted by chance.

The protein function prediction results are as follows: PF14_0697 is identified as a conserved hypothetical protein with a homodimeric type dihydroorotase function, receiving a high score of 0.999. PfOPRT is predicted to be a hypothetical protein similar to orotate phosphoribosyltransferase, also with a score of 0.999. Furthermore, atcasE is associated with aspartate carbamoyltransferase and aspartate transcarbamoylase, belonging to the ATCase/OTCase family, with a slightly lower but still substantial score of 0.991 (Table 2). These scores reflect the confidence in the predicted functions, with higher scores indicating a more reliable prediction. The identified functions encompass enzymes that contribute to the pyrimidine nucleotide synthesis, contributing valuable insights into the molecular processes of *P. falciparum*.

The Gene Ontology (GO) enrichment analysis highlighted the significant involvement of *P. falciparum* dihydroorotate dehydrogenase in various Biological Processes (BP) related to pyrimidine metabolism. The GO term "GO:0019856-Pyrimidine nucleobase biosynthetic process" exhibited a high prediction strength of 2.63, accompanied by an exceptionally low False Discovery Rate (FDR) of 6.41E-14, indicating a robust correlation. Similarly, "GO:0006207-De novo pyrimidine nucleobase biosynthetic process" and "GO:0044205-De novo UMP biosynthetic process" demonstrated prediction strengths of 2.61, with FDRs of 8.79E-10. Other relevant terms, such as "GO: 0009130-Pyrimidine nucleoside monophosphate biosynthetic process," "GO:0009220-Pyrimidine ribonucleotide biosynthetic process," "GO:0006221-Pyrimidine nucleotide biosynthetic process," and "GO:0009123-Nucleoside monophosphate metabolic process," exhibited prediction strengths ranging from 2.1 to 2.53 and FDR values ranging from 1.33E-11 to 7.56E-15

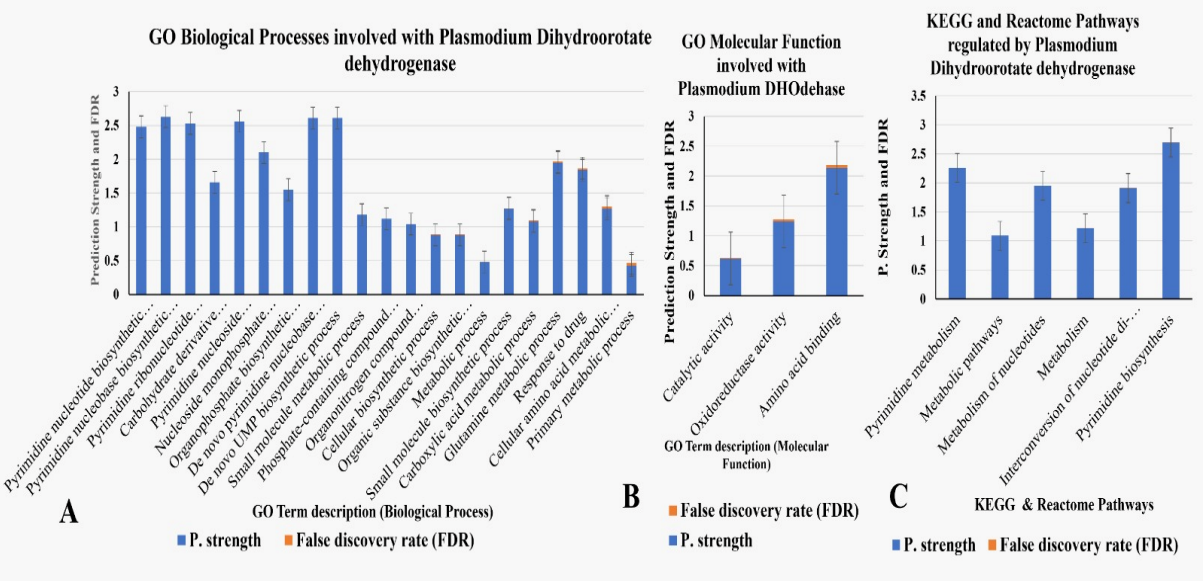

Figure 10: The bar graph of statistically significant GO terms of (A) Biological process, (B) Molecular function and (C) statistically significant KEGG and Reactome pathways influenced by Dihydroorotate dehydrogenase of *Plasmodium falciparum* that induces the metabolism of dihydroorotate into orotate during Pyramidine synthesis pathways.

(Figure 10 A). These results give information on the specific biological processes involved with DHOdehase in the framework of pyrimidine metabolism.

P. falciparum DHOdehase has a variety of functional activities, as shown by the GO enrichment analysis for Molecular Functions (MF). Although it had a comparatively greater FDR of 0.0468, the GO: 0016597 for amino acid binding showed a significant correlation with amino acid binding with a prediction strength of 2.14. Furthermore, with an FDR of 0.0314, the GO term GO: 0016491 for oxidoreductase activity demonstrated a prediction strength of 1.24, indicating involvement in redox reactions. The more extensive GO term GO: 0003824 for Catalytic activity revealed a prediction strength of 0.62, showing an overall catalytic function, followed by a low FDR of 0.00018 (Figure 10 B). The aforementioned findings offer an in-depth analysis of the molecular roles linked to DHOdehase, which include amino acid binding, oxidoreductase activity and further catalytic functions.

The analysis of pathway enrichment also demonstrated noteworthy correlations between *P. falciparum* DHOdehase and other important metabolic pathways. Pyrimidine metabolism's KEGG term map00240 showed a strong association with a high prediction strength of 2.26 and an exceptionally low FDR of 8.39E-11. Furthermore, map01100 for metabolic pathways demonstrated a 1.09 prediction strength with a 0.00013 FDR, highlighting its significance for the target protein's metabolic processes. Notable prediction strengths ranging from 1.22 to 2.69 and FDR values ranging from 8.60E-06 to 0.0027 were also displayed by specific KEGG terms PFA-15869 for Metabolism of Nucleotides, PFA-1430728 for Metabolism, PFA-499943 for Interconversion of Nucleotide Di- and Triphosphates and PFA-500753 for Pyrimidine Biosynthesis (Figure 10 C). These results offer a thorough understanding of the possible contribution of dihydroorotate dehydrogenase to important metabolic processes in *P. falciparum*.

Isothermal Titration Calorimetry (ITC)

The model was fitted with the results and the number of binding sites (n), floating association constant (ka) and binding enthalpy (ΔH) were used to measure the affinity between Dihydroorotate Dehydrogenase and ligands (Artemisinin and derivatives Artemisitene, Artemether, Artemotil, Dihydroartemisinin or Artenimol and Artesunate). The ITC measurement data unequivocally shows that Dihydroorotate Dehydrogenase has a higher affinity for the compound's artemisinin and its stereo isomer artesunate than it does for the other ligands (stereoisomers of artemisinin) that were used in this study, such as artemisitene, arttemether, artemotil, dihydroartemisinin, or artenimol. Compound Artemisinin and its stereoisomer Artesunate exhibited a higher affinity, as evidenced by their affinity parameter (defined by the ITC) of floating association constant (Ka), which was reported to be 6.12x106 and 5.96x106, respectively, their binding enthalpy (ΔH) of -46.32 and -44.65 kl/mol and their higher binding sites (n), 1.76 and 1.64 (Table 3). The Table 4 presents the results of isothermal titration calorimetry measurements, detailing the binding constants between Dihydroorotate Dehydrogenase and various ligands (Artemisinin and its derivatives: Artemisitene, Artemether, Artemotil, Dihydroartemisinin or Artenimol and Artesunate) at 25°C and pH 7.5 (Figure 11).

The aforementioned discoveries bolster the in-silico forecast employed in the search for affinity between Dihydroorotate

Table 2: DHOdehase induces the metabolism of dihydroorotate into orotate in *P. falciparum* and interacts with ten functional Partner proteins with high score as revealed by STRING Data base version 11.5.

Protein Symbol	Description	Score
PF14_0697	Conserved hypothetical protein; Dihydroorotase, homodimeric type; Dihydroorotase.	0.999
PfOPRT	Hypothetical protein similar to orotate phosphoribosyltransferase.	0.999
atcasE	Aspartate carbamoyltransferase and Aspartate transcarbamoylase which belong to the ATCase/ OTCase family.	0.991
DHFR-TS	Thymidylate synthase, a bifunctional dihydrofolate reductase, is involved in de novo dTMP production. A key enzyme in folate metabolism.	0.973
cpsSII	Hypothetical protein similar to carbamoyl-phosphate synthase large subunit.	0.961
PF14_0100	Cytidine triphosphate synthase promotes the ATP-dependent amination of UTP to CTP, using either L-glutamine or ammonia as a nitrogen source.	0.957
PF13_0353	Conserved hypothetical protein like NADH-cytochrome B5 reductase, putative.	0.930
PFA_0555c	Conserved hypothetical protein like UMP-CMP kinase, putative	0.920
PFF0740c	Putative Gpi-anchored wall transfer protein 1.	0.906
PF11_0407	Conserved hypothetical proteins like NADPH-adrenodoxin oxidoreductase, putative; mitochondrial	0.889

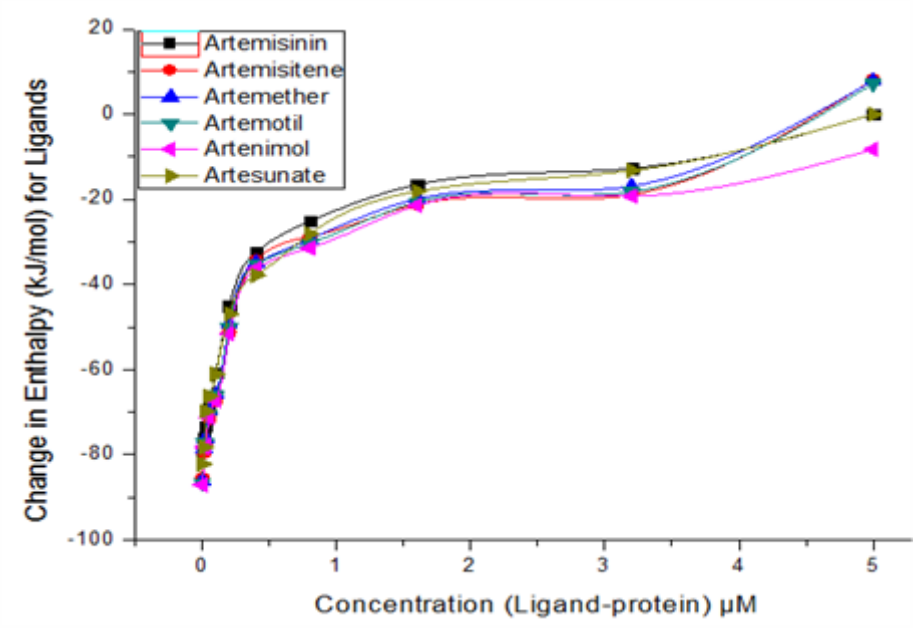

Figure 11: Figure depicts isothermal titration calorimetry measurement determination of the Binding Constant of between Dihydroorotate Dehydrogenase and ligands (Artemisinin and derivatives Artemisitene, Artemether, Artemotil, Dihydroartemisinin or Artenimol and Artesunate) at 25°C, pH 7.5.

Table 3: **Table summarizes the ITC measurements towards binding affinity between Dihydroorotate Dehydrogenase and ligands (Artemisinin and derivatives Artemisitene, Artemether, Artemotil, Dihydroartemisinin or Artenimol and Artesunate) at 25°C, pH 7.5.**

Ligands	Floating association constant ka (1/M)	Binding enthalpy ΔH (kJ/mol)	Binding sites (n)
Artemisinin	$6.12x10^6$	-46.32	1.76
Artemisitene	$5.54x10^4$	-53.34	1.23
Artemether	$5.89x10^4$	-54.31	1.18
Artemotil	$6.54x10^4$	-54.49	1.21
Artenimol	$5.23x10^4$	-53.78	1.16
Artesunate	$5.96x10^6$	-44.65	1.64

Table 4: **Table summarizes the isothermal titration calorimetry measurement determination of the Binding Constant of between Dihydroorotate Dehydrogenase and ligands (Artemisinin and derivatives Artemisitene, Artemether, Artemotil, Dihydroartemisinin or Artenimol and Artesunate) at 25°C, pH 7.5.**

Concentration	ΔH (kJ/mol) for Ligands					
Ligand/ protein (μM)	Artemisinin	Artemisitene	Artemether	Artemotil	Artenimol	Artesunate
0.0125	-76.09	-79.52	-78.67	-77.19	-78.29	-78.21
0.025	-73.31	-77.23	-76.21	-77.12	-77.87	-69.76
0.050	-68.38	-71.53	-69.65	-70.56	-71.28	-66.23
0.100	-60.80	-67.21	-65.70	-66.11	-67.32	-61.11
0.200	-45.11	-51.16	-49.10	-50.12	-51.60	-46.90
0.400	-32.32	-34.28	-34.87	-35.21	-36.26	-37.81
0.800	-25.11	-28.78	-29.31	-30.32	-31.41	-28.12
1.600	-16.51	-21.11	-19.87	-20.65	-21.41	-18.11
3.20	-12.70	-18.86	-16.87	-18.20	-19.20	-13.22
5.00	00	08.10	07.89	07.21	-08.22	00

Dehydrogenase and Artemisinin, as well as their derivatives, Artemisitene, Artemether, Artemotil, Dihydroartemisinin, or Artenimol and Artesunate. Compound Artemisinin and its steroisomer Artesunate were shown to have relatively improved stability and to retain many of the interactions seen during XP docking earlier in the investigation. The top hit compound in the investigation was determined to be artemisinin and its steroisomer artesunate, based on docking. Due to different forms of interactions with Dihydroorotate Dehydrogenase's, the ligands (Artemisinin and its steroisomer Artesunate) had a higher affinity than the other ligands (Artemisitene, Artemether, Artemotil, Dihydroartemisinin, or Artenimol), as described in the insilico studies. Additional ligand molecules, such as artemisitene, artemotil, dihydroartemisinin, or artenimol, also demonstrated encouraging affinity for the enzyme dihydroorotate dehydrogenase and may be considered as candidates for further research and development.

DISCUSSION

To address the global health challenge, the discussion begins by acknowledging the gravity of malaria as a widespread illness that affects millions of individuals, particularly in tropical and subtropical regions. The high incidence rates reported by the WHO underscore the urgent need for innovative approaches to combat the malaria. Malaria, affecting 300-500 million people annually worldwide, leads to approximately 2 million fatal infections happened by the *P. falciparum*, that is transmitted by Anopheles mosquitoes.[4] The study focuses on Artemisinin, a compound derived from the *Artemisia annua* plant, renowned for its potent antimalarial properties. Its peculiar sesquiterpene lactone structure with an endoperoxide (-O-O-) bridge has been well-documented for its efficacy against Plasmodium parasites.[32,33] *Artemisia annua* is the sole plant containing artemisinin in quantities (0.01-0.8% dry weight) suitable for commercial utilization. In treating multidrug-resistant malaria, artemisinin and its derivatives prove highly effective, supplanting other drugs derived from natural sources that have lost efficacy.[34] The recognition of Artemisinin's importance sets the stage for a deeper exploration of its stereoisomers. A crucial aspect of the study is

the detailed exploration of Artemisinin's fourteen stereoisomers and their potential docking activities. The acknowledgment of optical isomerism due to chiral centers introduces a level of complexity that the research aims to unravel. Understanding the distinct activities of these stereoisomers is pivotal for drug development, providing insights into their potential therapeutic efficacy against the Plasmodium parasite.

The current study represents a significant step in the ongoing efforts to combat malaria, a major global health challenge. By focusing on the computational exploration of Artemisinin stereoisomers and their derivatives showing interactions with key pathogenic proteins of Plasmodium parasite- Dihydroorotate dehydrogenase (DHOdehase), will expand the horizon to the drug discovery field. The identification of specific pathogenic proteins, including Sarcoplasmic/endoplasmic reticulum calcium ATPase (ATP2A), Exported antigen AG 5.1 (EXP-1), Elongation factor 1-alpha 1 (MEF-1) and Beta-Hematin Formation (BHF), underscores the targeted approach of the study. The distinction between the infection phases in the liver and blood draws attention to how complex the Plasmodium life cycle is. These proteins are attractive targets for developing antimalarial drugs because they are important at several stages of Plasmodium life cycle. The study highlights how crucial it is to interfere with these essential metabolic pathways and cellular functions to effectively treat and prevent malaria.

The present discourse elucidates the consequences and possibilities of Artemisinin Stereoisomers directed towards the plasmodium parasite DHOdehase, a protein that performs molecular docking. The study examines the molecular and atomic interactions between the artemisinin stereoisomers and important amino acid residues of the Plasmodium parasite DHOdehase.

When combined with network biology techniques, molecular docking offers a comprehensive picture of possible drug-target interactions. The comprehension of the complex molecular mechanisms behind artemisinin's antimalarial action is improved by this integrated method. The proteins found in our investigation are crucial interactors during the invasion of hepatocytes and infection of blood stages. By focusing on these proteins, one can strategically interrupt the parasite life cycle at various critical points. Artemisinin and its stereoisomer displayed distinct patterns of affinity and interaction with the target enzyme, Dihydroorotate dehydrogenase, as observed in the ITC experiment. These differences are primarily attributed to structural variations in how the drug binds to Dihydroorotate dehydrogenase. Kung *et al.* (2010) demonstrated that optimizing the chiral center of Artemisinin can yield a new class of highly effective compounds.[35] Similarly, Peter *et al.* (2021) reported on effective hybrid compounds derived from Artemisinin and its derivatives for cancer and malaria treatment, achieved by modifying the chiral center.[36]

The significance of comprehending the interactions between the stereoisomers of artemisinin and the Plasmodium parasite DHOdehase is emphasized as the discussion concludes. Potential preclinical research as well as additional experimental validations can be made possible by identifying molecular and atomic interactions. The results of the investigation provide promise for the generation of potent antimalarial medications that can interrupt the parasite life cycle and treat malaria.

CONCLUSION

To sum up, our computational investigation of the stereoisomers of artemisinin is a comprehensive and exhaustive method of deciphering the subtleties of their interactions with the Plasmodium parasite's DHOdehase. Of the fourteen stereoisomers of artemisinin, two, C6 and C8, potentially formed hydrogen bonds, alkyl/Pi-alkyl, carbon-hydrogen bond, Pi-Sigma and Van der Waals interactions with Plasmodium DHOdehase through significant negative docking energy. The ITC findings clearly demonstrate the varying affinities of Dihydroorotate dehydrogenase (DHOdehase) for Artemisinin and its derivatives, which are influenced by changes in the chiral centers. The differences in enthalpy (ΔH) observed in the ITC experiment among the chiral center-based Artemisinin derivatives also suggest a potential correlation with the efficacy of anti-malarial drug candidates. This stereochemical structural variety implies potential changes in the pharmacological actions of Artemisinin, a crucial concern in medication development. Investigating these stereoisomers provides opportunities to comprehend their unique functions in interfering with the Plasmodium life cycle. The outcomes not only expand knowledge of the molecular underpinnings of antimalarial action but also lay the groundwork for upcoming efforts to create drugs in the battle against malaria.

ACKNOWLEDGEMENT

The author gratefully acknowledges the funding of the Deanship of Graduate Studies and Scientific Research, Jazan University, Saudi Arabia, through Project Number (RG24-M017).

CONFLICT OF INTEREST

The author declares that there is no conflict of interest.

FUNDING

Deanship of Graduate Studies and Scientific Research, Jazan University, Saudi Arabia, Project Number (RG24-M017).

ABBREVIATIONS

DHOdehase: Dihydroorotate dehydrogenase; **STRING:** Search Tool for the Retrieval of Interacting Genes/Proteins; **DB:** Database; **KEGG:** Kyoto Encyclopedia of Genes and Genomes; **ITC:** Isothermal Titration Calorimetry; **WHO:** World Health

Organization; **HBV:** Hepatitis B Virus; **ACTs:** Artemisinin-Based Combination Therapies; **RBC:** Red Blood Cell; **EMA:** European Medicines Agency; **TDD:** Therapeutic Target Database; **UMP:** Uridine Monophosphate; **FMN:** Flavin Mononucleotide; **NAD:** Nicotinamide Adenine Dinucleotide; **NADP:** Nicotinamide Adenine Dinucleotide Phosphate; **PMV:** Python Molecular Viewer; **SDF:** Structure Data File; **SMILES:** Simplified Molecular Input Line Entry System; **SAR:** Structure-Activity Relationships; **QSAR:** Quantitative Structure-activity Relationships; **BLASTp:** Basic Local Alignment Search Tool for proteins; **BLOSUM62:** Blocks Substitution Matrix 62; **PDB:** Protein Data Bank; **VDW:** van der Waals; **PPI:** Protein-Protein Interaction; **GGI:** Gene-Gene Interactions; **GO:** Gene Ontology; **Pfam:** Protein Families; **CC:** Cellular Component; **BP:** Biological Process; **MF:** Molecular Function; **FDR:** False Discovery Rate; **HEPES:** (4-(2-hydroxyethyl)-1-piperazineethanesulfonic acid.

SUMMARY

This study explores the interactions between Plasmodium Dihydroorotate dehydrogenase (DHOdehase) and Artemisinin, focusing on its fourteen stereoisomers, which differ due to their seven chiral centers. Using computational techniques like molecular docking and network pharmacology, the researchers identified key binding sites at the C6 and C8 positions of the stereoisomers, showing strong interactions with DHOdehase (binding energies of -8.7 and -8.2 kcal/mol). The interactions involve hydrogen bonds, Van der Waals forces and Pi-Sigma bonds. STRING DB network analysis revealed DHOdehase's interactions with 10 functional partner proteins, while pathway enrichment linked DHOdehase to pyrimidine metabolism. Isothermal Titration Calorimetry (ITC) confirmed higher binding affinities for Artemisinin and Artesunate. These findings provide a foundation for further experimental validation and potential antimalarial drug development.

REFERENCES

1. M'Bra RK, Kone B, Soro DP, N'krumah RT, Soro N, Ndione JA, *et al.* Impact of climate variability on the transmission risk of malaria in northern Côte d'Ivoire. PLOS ONE. 2018;13(6):e0182304. doi: 10.1371/journal.pone.0182304, PMID 29897901.
2. Snow RW. Global malaria eradication and the importance of Plasmodium falciparum epidemiology in Africa. BMC Med. 2015;13(1):23. doi: 10.1186/s12916-014-0254-7, PMID 25644195.
3. Garcia LS. Malaria. Clin Lab Med. 2010;30(1):93-129. doi: 10.1016/j.cll.2009.10.001, PMID 20513543.
4. World malaria report 2023. Published online; 2023. p. 1-356.
5. Boss C, Aissaoui H, Amaral N, Bauer A, Bazire S, Binkert C, *et al.* Discovery and characterization of ACT-451840: an antimalarial drug with a novel mechanism of action. ChemMedChem. 2016;11(18):1995-2014. doi: 10.1002/cmdc.201600298, PMID 27471138.
6. Breman JG. Eradicating malaria. Sci Prog. 2009;92(1):1-38. doi: 10.3184/003685009X440290, PMID 19544698.
7. Olliaro PL, Haynes RK, Meunier B, Yuthavong Y. Possible modes of action of the artemisinin-type compounds. Trends Parasitol. 2001;17(3):122-6. doi: 10.1016/S1471-4922(00)01838-9, PMID 11286794.
8. Shi C, Li H, Yang Y, Hou L. Anti-inflammatory and immunoregulatory functions of artemisinin and its derivatives. Mediators Inflamm. 2015; 2015:435713. doi: 10.1155/2015/435713, PMID 25960615.
9. Lee J, Zhou HJ, Wu XH. Dihydroartemisinin downregulates vascular endothelial growth factor expression and induces apoptosis in chronic myeloid leukemia K562 cells. Cancer Chemother Pharmacol. 2006;57(2):213-20. doi: 10.1007/s00280-005-0002-y, PMID 16075280.
10. Efferth T, Romero MR, Wolf DG, Stamminger T, Marin JJ, Marschall M. The antiviral activities of artemisinin and artesunate. Clin Infect Dis. 2008;47(6):804-11. doi: 10.1086/591195, PMID 18699744.
11. Eastman RT, Fidock DA. Artemisinin-based combination therapies: a vital tool in efforts to eliminate malaria. Nat Rev Microbiol. 2009;7(12):864-74. doi: 10.1038/nrmicro2239, PMID 19881520.
12. Baldwin J, Farajallah AM, Malmquist NA, Rathod PK, Phillips MA. Malarial dihydroorotate dehydrogenase. Substrate and inhibitor specificity. J Biol Chem. 2002;277(44):41827-34. doi: 10.1074/jbc.M206854200, PMID 12189151.
13. Heikkilä T, Ramsey C, Davies M, Galtier C, Stead AM, Johnson AP, *et al.* Design and synthesis of potent inhibitors of the malaria parasite dihydroorotate dehydrogenase. J Med Chem. 2007;50(2):186-91. doi: 10.1021/jm060687j, PMID 17228860.
14. Choi SR, Mukherjee P, Avery MA. The fight against drug-resistant malaria: novel plasmodial targets and antimalarial drugs. Curr Med Chem. 2008;15(2):161-71. doi: 10.2174/092986708783330575, PMID 18220771.
15. Phillips MA, Rathod PK. Plasmodium dihydroorotate dehydrogenase: A promising target for novel anti-malarial chemotherapy. Infect Disord Drug Targets. 2010;10(3):226-39. doi: 10.2174/187152610791163336, PMID 20334617.
16. Fagan RL, Nelson MN, Pagano PM, Palfey BA. Mechanism of flavin reduction in Class 2 dihydroorotate dehydrogenases. Biochemistry. 2006;45(50):14926-32. doi: 10.1021/bi060919g, PMID 17154530.
17. Nara T, Hshimoto T, Aoki T. Evolutionary implications of the mosaic pyrimidine-biosynthetic pathway in eukaryotes. Gene. 2000;257(2):209-22. doi: 10.1016/S0378-1119(00)00411-X, PMID 11080587.
18. Hines V, Keys LD, Johnston M. Purification and properties of the bovine liver mitochondrial dihydroorotate dehydrogenase. J Biol Chem. 1986;261(24):11386-92. doi: 10.1016/S0021-9258(18)67396-X, PMID 3733756.
19. Li YH, Li XX, Hong JJ, Wang YX, Fu JB, Yang H, *et al.* Clinical trials, progression-speed differentiating features and swiftness rule of the innovative targets of first-in-class drugs. Brief Bioinform. 2020;21(2):649-62. doi: 10.1093/bib/bby130, PMID 30689717.
20. Tian W, Chen C, Lei X, Zhao J, Liang J. CASTp 3.0: computed atlas of surface topography of proteins. Nucleic Acids Res. 2018;46(W1):W363-7. doi: 10.1093/nar/gky473, PMID 29860391.
21. Trott O, Olson AJ. AutoDock Vina: improving the speed and accuracy of docking with a new scoring function, efficient optimization and multithreading. J Comput Chem. 2010;31(2):455-61. doi: 10.1002/jcc.21334, PMID 19499576.
22. Seeliger D, de Groot BL. Ligand docking and binding site analysis with PyMOL and Autodock/Vina. J Comput Aid Mol Des. 2010;24(5):417-22. doi: 10.1007/s10822-010-9352-6, PMID 20401516.
23. Morris GM, Huey R, Lindstrom W, Sanner MF, Belew RK, Goodsell DS, *et al.* AutoDock4 and AutoDockTools4: automated docking with selective receptor flexibility. J Comput Chem. 2009;30(16):2785-91. doi: 10.1002/jcc.21256, PMID 19399780.
24. Elkhalifa AE, Al-Shammari E, Kuddus M, Adnan M, Sachidanandan M, Awadelkareem AM, *et al.* Structure-based multi-targeted molecular docking and dynamic simulation of soybean-derived isoflavone genistin as a potential breast cancer signaling proteins inhibitor. Life (Basel). 2023;13(8):1739. doi: 10.3390/life13081739, PMID 37629596.
25. Ashraf SA, Elkhalifa AE, Mehmood K, Adnan M, Khan MA, Eltoum NE, *et al.* Multi-targeted molecular docking, pharmacokinetics and drug-likeness evaluation of okra-derived ligand abscisic acid targeting signaling proteins involved in the development of diabetes. Molecules. 2021;26(19):5957. doi: 10.3390/molecules26195957, PMID 34641501.
26. Laskowski RA, Swindells MB. LigPlot+: multiple ligand-protein interaction diagrams for drug discovery. J Chem Inf Model. 2011;51(10):2778-86. doi: 10.1021/ci200227u, PMID 21919503.
27. Schrödinger LL. The {PyMOL} Molecular Graphics System, Version~1.8; 2015.
28. Szklarczyk D, Gable AL, Nastou KC, Lyon D, Kirsch R, Pyysalo S, *et al.* The STRING database in 2021: customizable protein-protein networks and functional characterization of user-uploaded gene/measurement sets. Nucleic Acids Res. 2021;49(D1):D605-12. doi: 10.1093/nar/gkaa1074, PMID 33237311.
29. Baig MS, Krishnan A. A bioinformatics approach to investigate serum and hematopoietic cell-specific therapeutic microRNAs targeting the 3' UTRs of all four dengue virus serotypes. Pathog Dis. 2021;79(8). doi: 10.1093/femspd/ftab050, PMID 34610125.
30. Baig MS, Deepanshu PP, Alam P, Krishnan A. In silico analysis reveals hypoxia-induced miR-210-3p specifically targets SARS-CoV-2 RNA. J Biomol Struct Dyn. Published online February 8, 2023. 2023;41(21):1-23. doi: 10.1080/07391102.2023.2175255, PMID 36752331.
31. Vanselow NR, Bourret JC. Online interactive tutorials for creating graphs with excel 2007 or 2010. Behav Anal Pract. 2012;5(1):40-6. doi: 10.1007/BF03391816, PMID 23326629.
32. Alam P, Abdin MZ. Over-expression of HMG-CoA reductase and amorpha-4,11-diene synthase genes in Artemisia annua L. and its influence on artemisinin content. Plant Cell Rep. 2011;30(10):1919-28. doi: 10.1007/s00299-011-1099-6, PMID 21655998.

33. Woerdenbag HJ, Lugt CB, Pras N. Artemisia annua L.: a source of novel antimalarial drugs. Pharm Weekbl Sci. 1990;12(5):169-81. doi: 10.1007/BF01980041, PMID 2255584.
34. Van Geldre E, Vergauwe A, Van den Eeckhout E. State of the art of the production of the antimalarial compound artemisinin in plants. Plant Mol Biol. 1997;33(2):199-209. doi: 10.1023/a:1005716600612, PMID 9037139.
35. Kung SH, Lund S, Murarka A, McPhee D, Paddon CJ. Approaches and recent developments for the commercial production of semi-synthetic artemisinin. Front Plant Sci. 2018;9:87. doi: 10.3389/fpls.2018.00087, PMID 29445390.
36. Peter S, Jama S, Alven S, Aderibigbe BA. Artemisinin and derivatives-based hybrid compounds: promising therapeutics for the treatment of cancer and malaria. Molecules. 2021;26(24):7521. doi: 10.3390/molecules26247521, PMID 34946603.

Cite this article: Rehman Z. Strategic Targeting of Plasmodium Dihydroorotate Dehy-drogenase through Antimicrobial Artemisinin Chiral Cen-ters and their Derivatives: An Integrative Study Using Network Pharmacology and Isothermal Titration Calo-rimetry. Indian J of Pharmaceutical Education and Research. 2024;58(4):1356-72.